

SODA INCORPORATION DURING HYDRATE PRECIPITATION

Chris Vernon, Joanne Loh, Daniel Lau & Andrew Stanley

AJ Parker CRC for Hydrometallurgy (CSIRO Minerals); PO Box 90, Bentley WA 6982, Australia

Keywords: soda, gibbsite, hydrate, growth mechanism

Abstract

The economic necessity to achieve high precipitation yields and tough alumina must be balanced against another important quality consideration - occluded soda. Although there are a number of publications that develop hypotheses for the mechanism of soda incorporation, and some that give mathematical relationships to describe the rate of soda incorporation, none attempt to do this with any reference to known physical and chemical phenomena associated with the hydrate (gibbsite) growth mechanism.

The present work describes soda incorporation as a function of growth rate and develops a hypothesis that crystal defects are trapping sites for sodium ions. The incorporation of sodium ions into gibbsite crystals is a direct consequence of the growth mechanism. A mathematical model for incorporation is developed along basic statistical mechanical principles and the contribution of organic carbon towards defect generation is explored.

Introduction

Despite its ubiquity, soda remains an enigmatic impurity in hydrate. It is empirically well understood that low temperature and high supersaturation both contribute to higher soda levels. It is also well known that some organic carbon impurities may also cause a higher level of incorporation. However, there is no consensus on how sodium becomes part of the crystal or where it resides. Bayer liquors typically contain 4 to 6 mol L⁻¹ sodium ions and perhaps one of the most interesting aspects of soda incorporation is not that *so much* sodium becomes incorporated, but, considering the overwhelming amount of sodium present, that *so little* does.

Wefers [1] suggested that sodium ions are atomically dispersed in the crystal lattice. Sang [2] largely agrees, showing that liquor occlusions could not possibly explain soda incorporation. Eremin [3, 4] hypothesized that sodium is included in the interlayer hydroxyl gaps of the structure, by isomorphous substitution of hydrogen in the OH groups. However, none of these authors suggest the mechanism whereby sodium enters the crystal.

Grocott and Rosenberg [5] do suggest that the mechanism involves the trapping of sodium ions in a growing layer of gibbsite. These sodium ions do not come directly from Bayer liquor. Rather they result from polymerisation of sodium aluminate that occurs during the hydrate precipitation reaction. If the sodium ions do not have time to diffuse away from the growing hydrate surface, they can be incorporated into the hydrate crystal structure, thereby giving rise to soda in alumina. A comparable hydrate growth mechanism has been suggested by Gerson [6] although speciation measurements in Bayer liquors [7-9] and direct observation of growing gibbsite surfaces [10] do not agree with the surface polymer model *per se*.

Whatever the location of soda in the lattice and the mechanism of its incorporation, few authors have described models for predicting soda levels based on various parameters. Sang [2] found a strong correlation with supersaturation as shown in Equation 1:

$$\frac{dNa_2O}{dAl_2O_3} = a(A - A_e)^2 \quad (1)$$

Where A_e is the equilibrium alumina concentration. Sang found that a was a function of liquor composition. Clerin and Cristol [11] found that temperature was not a significant factor – only supersaturation and to a lesser extent, humates. Armstrong *et al.* [12, 13] found an effect of temperature, supersaturation and organic carbon, re-writing Sang's equation as:

$$\frac{dNa_2O}{dAl_2O_3} = a'' \left(\frac{A}{C} - \frac{A}{C_\infty} \right)^2 \quad (2)$$

a'' was fitted for a number of different liquor compositions:

$$a'' = (0.000598 \times C) - (0.00036 \times T) + (0.019568 \times \frac{TOOC}{C}) \quad (3)$$

where C is caustic (expressed as g L⁻¹ Na₂CO₃ equivalent), T is temperature (°C) and TOOC is total oxidisable organic carbon, otherwise referred to in the present work as TOC. Armstrong's equation clearly shows a small positive dependency on caustic concentration, a larger positive dependency on TOC, and a small negative dependency on temperature. As with all empirically derived equations, the expression for a'' should be treated with caution and will require tuning for each refinery where it is used.

In all of the previously published work, the different findings for whether or not there is a temperature effect could arise from the solubility correlation used. The temperature dependence used for the solubility prediction could have a profound effect on the perceived effect of temperature on sodium incorporation.

More recent developments in the understanding of the mechanism of gibbsite crystal growth can assist in understanding the mechanism of sodium incorporation. The incorporation of sodium occurs during gibbsite growth and is more than likely intimately connected with the mechanism of crystal growth. Vernon *et al.* [14] suggest that gibbsite grows by collapse of a pre-organized gibbsite-like association of aluminate ions both present in the liquor and adsorbed onto the surface. The rate of this collapse is governed by the relative populations of the clusters, which itself is a function of supersaturation, and determines the physical mechanism of growth. For low concentrations, well-ordered but slow addition at spiral defects occurs; for high concentrations, spontaneous surface nucleation occurs [15, 16]. The hypothesis is consistent with all known

growth and solution speciation phenomena. Such mechanistic hypotheses provide significant theoretical underpinning in understanding soda incorporation.

Experimental

Experiments were conducted both at constant supersaturation (and therefore fairly constant growth rate) and in batch experiments where growth rate did not vary much over the course of each run. Synthetic liquors were made using analytical grade sodium hydroxide and Alcoa C31 white hydrate. Carbonate levels were typically less than 2 g L^{-1} . Experimental runs were seeded with coarse ($+63 \mu\text{m}$) C31. In some of the experimental work, sodium D,L-tartrate, was added as a model hydrate active organic.

Constant Composition Experiments

In order to maintain constant supersaturation, a reactor system was constructed where liquor conductivity could be monitored constantly. Precipitation of hydrate increases the conductivity (hydroxide ions are more mobile than aluminate ions). LabView™ software, running on a PC, was used to detect the change in conductivity and in response to this, to remove an aliquot of the liquor, replacing it with more supersaturated liquor. The resulting system maintained the alumina concentration constant within $0.2 \text{ g L}^{-1} \text{ Al}_2\text{O}_3$. Figure 1 shows a schematic of the apparatus used.

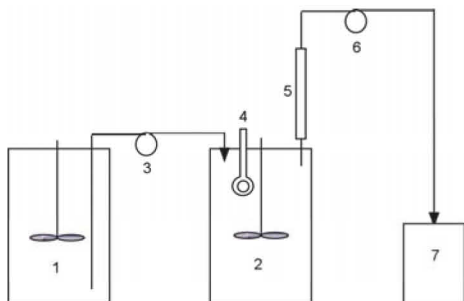


Figure 1. A schematic representation of the reactor hardware, including thermostatically controlled 4 litre green liquor tank (1) and 4 litre reactor (2), feed pump (3), conductivity probe (4), solids retention tube (5), liquor removal pump (6) and waste vessel (7).

Batch Experiments

To compliment the constant composition experiments in the low growth rate parts of the work, longer-term batch experiments were conducted. Difficulties can arise when attempting to reconcile the results of batch precipitations with constant composition precipitation because batch experiments tend to experience a wide range of supersaturations. In theory this can be accounted for by integration with respect to alumina concentration, but this approach assumes accurate knowledge of the growth mechanism and sodium incorporation mechanism. Rather than rely on a possibly faulty assumption in this regard, batch experiments were devised where the supersaturation did not vary significantly. This was accomplished by using a low seed loading and frequent decanting of liquor and topping up with fresh liquor. In this way the alumina concentration did not vary by more than $3 \text{ g L}^{-1} \text{ Al}_2\text{O}_3$ during each experiment. While this does introduce an error

greater than that experienced for the constant composition experiments, it is still acceptable.

Spectroscopy

In order to understand more about the mechanisms of sodium incorporation, a wide variety of spectroscopic methods were applied, including $^{23}\text{NaMAS-NMR}$, EXAFS, SANS and dielectric relaxation.

Mechanism and Location Findings

Building on the work and models of Gale [17], *ab initio* molecular modeling suggests that sodium ions should be able to replace certain protons in the lattice and that the energy difference incurred by this substitution is minimal – effectively agreeing with Eremin's suggestion of substitution for protons. However, all spectroscopic attempts failed to locate sodium in any crystallographically distinct location. Magic Angle Spinning solid state NMR spectroscopy shows a very broad ^{23}Na peak consistent with a disordered environment. Enhanced X-ray Absorption Fine Structure (EXAFS) indicated a wide variety of sodium environments, and none that could be positively identified. Similar findings emerged from high-resolution powder diffraction and from small angle neutron scattering. In short, all techniques that could identify a single, or a group of, dominant locations, failed. This is sufficient evidence that either the sodium is highly mobile under all conditions (which is unlikely, particularly at liquid nitrogen temperatures used in $^{23}\text{NaMAS-NMR}$ experiments) or that the sodium is genuinely atomically dispersed. Sodium is likely to be in non-regular locations such as defects in the crystal. Since the defects are likely to vary from atom stacking faults through to mismatched plane boundaries, the range of possible soda locations is diverse.

It would not be unreasonable then to expect that incorporated sodium would vary in concentration in direct proportion to the defect density. Observations of the growing hydrate surface have been made in our laboratories and reveal that at least two growth mechanisms occur depending on supersaturation and temperature. At low supersaturations the surface grows by spreading of well-behaved spiral defects. The population of crystalline defects generated during growth is expected to be quite low in the spiral mechanism. At higher supersaturations the spiral mechanism gives way to a birth and spread growth pattern which is inherently more disordered. It is expected that the birth and spread mechanism is likely to be responsible for the creation of the majority of crystal defects. Lee [15, 16] observes a cross-over region in the mechanisms of growth at a supersaturation (defined as $(A - A^*)/A^*$) of approximately 0.81, which corresponds to an A/C value of approximately 0.42 at 60°C , with a caustic concentration of 200 g L^{-1} (expressed as Na_2CO_3). Figure 2 shows previously unpublished images generated using atomic force microscopy (AFM). The images illustrate very clearly the differences between the spiral and the birth and spread growth patterns.

In order to test the dislocation hypothesis, a variety of hydrate samples of different soda levels and different origins were fractured in a ball mill and then leached with deionised water. If sodium ions exist predominantly at defect sites and plane boundaries, and crystals preferentially fracture at these same sites, a disproportionate amount of sodium will be available for

leaching, compared to the surface area. The baseline theoretical amount of sodium that should leach, if the soda is homogeneously dispersed, was calculated by assuming that sodium could traverse three aluminate layers (10 Å) to enter the solution. It is then a trivial exercise to calculate the sodium present in this volume from the surface area and the initial soda value. 10 Å is likely to be an over estimate. Table I shows the predicted and observed leachable soda for a variety of samples. It is very clear that much more sodium is leached than would be the case if soda was completely homogeneously dispersed. Therefore, the hypothesis of location at defects and plane boundaries appears to be supported.

Despite potentially complicated breakage mechanisms, the data in Table I gives a surprising amount of information for such a simple experiment. There is reasonable correspondence between the observed/theoretical leached soda column and the surface area ratio for the low TOC samples. The sample grown from high TOC liquor has a much larger observed/theoretical value than would be anticipated from the increase in surface area. It might be expected that growth from a high-TOC liquor would result in a greater population of defects in the crystal. Sample E was obviously contaminated with incorporated organic compounds during growth, having a pale brown appearance.

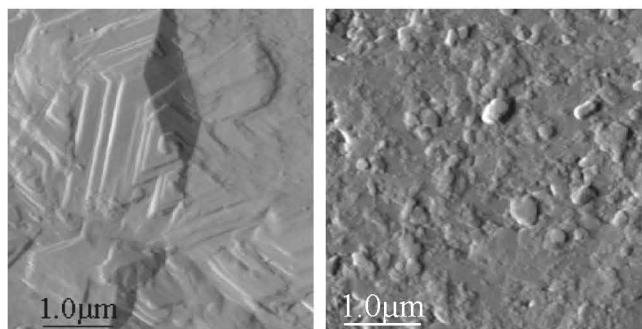


Figure 2. Atomic Force Microscopy reveals that under low supersaturation conditions, growth is *via* a well-ordered spiral mechanism (left) whereas under conditions of high supersaturation (right) growth is *via* surface nucleation and spread. (Images by kind permission of Felicia Lee, Curtin University, Western Australia)

Table I. Results for crushing and leaching of various hydrates. Soda is expressed as w/w Na₂O/Al₂O₃. Surface areas are m² g⁻¹ and were measured using the BET method. Before grinding or leaching, each sample was well washed a number of times with hot deionised water in order to remove washable soda. The leached concentrations of sodium were small and measured in the leach solution using atomic absorption spectroscopy. The theoretical leachable column refers to how much Na₂O would be expected to be extracted from the hydrate if the sodium was homogeneously dispersed and if ions could move 10 Å through the crystal. The observed/theoretical column shows the excess of sodium that can be leached beyond what is expected if soda was dispersed throughout the crystal. This excess probably reflects that soda is located primarily at defect sites.

Hydrate	Original % Na ₂ O	Original SA (m ² g ⁻¹)	Post-grind SA (m ² g ⁻¹)	SA ratio	Theoretical % Na ₂ O leachable	Observed % Na ₂ O leachable	Observed/Theoretical	Comments
A	0.417	0.07	1.27	18.0	0.00125	0.0090	7.15	Agglomerated. <i>No TOC</i>
B	0.242	0.30	1.68	5.6	0.00084	0.0047	5.54	Agglomerated. <i>Low TOC</i>
C	0.174	6.16	7.05	1.2	0.00038	0.00052	1.37	Small single crystals. <i>Low TOC</i>
D	0.275	0.02	1.02	51.0	0.00069	0.0174	25.4	Large single crystals. <i>Med. TOC</i>
E	0.278	0.08	1.00	12.5	0.00021	0.0066	30.7	Agglomerated. <i>High TOC</i>

General Form of the Equation

The initial difficulty in the interpretation of data, and the fitting of equations to describe soda incorporation, hinge around the lack of knowledge of the incorporation mechanism. Approaches such as Sang's at least pay some attention to the possibility of incorporation being proportional to growth rate [2]. In the search for appropriate mechanisms and models, the work of Hall [18] on semiconductor growth is appropriate if the mechanism of incorporation involves trapping of impurities by a growth front, as suggested by Grocott and Rosenberg [5]. Further, Hall's equation was adapted by Tsuchiyama *et al.* [19] to describe impurity incorporation in crystals grown from aqueous systems. The present equation was further developed from the work of those authors and follows a general statistical thermodynamic approach to the trapping of impurities and/or the generation of defects in a growing crystal, dependent on the surface population of impurity,

the rate of diffusion of the impurity away from the growth face, and the rate of growth.

The general form of the equation is:

$$\%Na_2O = f(eq, T) + f(N_{ads}, T, R_G, R_C) \quad (4)$$

Where *eq* is the equilibrium defect population and effectively the "solubility" of sodium in the crystal at temperature *T*. *N_{ads}* is the number density of sodium ions adsorbed onto growth sites, *R_G* is the rate of linear crystal growth and *R_C* is the critical growth rate, below which little sodium is trapped. Equation 4 seems to make good sense particularly in view of recent hypotheses for hydrate growth. The additional attraction of Equation 4 is that it expresses soda as a function of growth rate, rather than supersaturation. While supersaturation is fairly easy to calculate, it is sometimes in error (depending on the quality of the solubility calculation) and growth rate is influenced by surface area, induction times before

the onset of precipitation, and a number of other factors. Therefore, the measured growth rate was considered to be a more reliable measure for the present work.

Data Fitting

Equation 4 can be re-written using common relationships for equilibrium conditions and the kinetic relationship observed by Hall [18]. Equation 5 is one possible version of this:

$$\%Na_2O = k_{eq}e^{-E_{eq}/RT} + k_{ads}e^{-E_{ads}/RT}e^{-R_c/R_G} \quad (5)$$

Equation 5 essentially describes a family of S-shaped curves commencing with low sodium incorporation at low growth rates until a critical rate is approached, after which the sodium level increases through an almost linear zone until a plateau value is reached.

The results of both constant supersaturation and short supersaturation range batch experiments are shown in Figure 3. All data shown in Figure 3 was generated in liquors with caustic concentrations of $201 \pm 1.5 \text{ g L}^{-1}$ (as Na_2CO_3 equivalent). The findings conform to the general findings in the literature by various authors in that higher growth rates (i.e. higher supersaturations) and lower temperatures result in higher sodium incorporation. The novelty in the present data is in the broad range of growth conditions used, and the appearance of a plateau in the amount of sodium that can be incorporated at high growth rates. The fitted lines were generated using Equation 5 and the fit is good over the very large range of growth rates examined. It should be noted that a larger range of growth rates than can be found in an alumina refining situation were tested so that the quality of fit of the equation and fundamental usefulness of the equation could be tested.

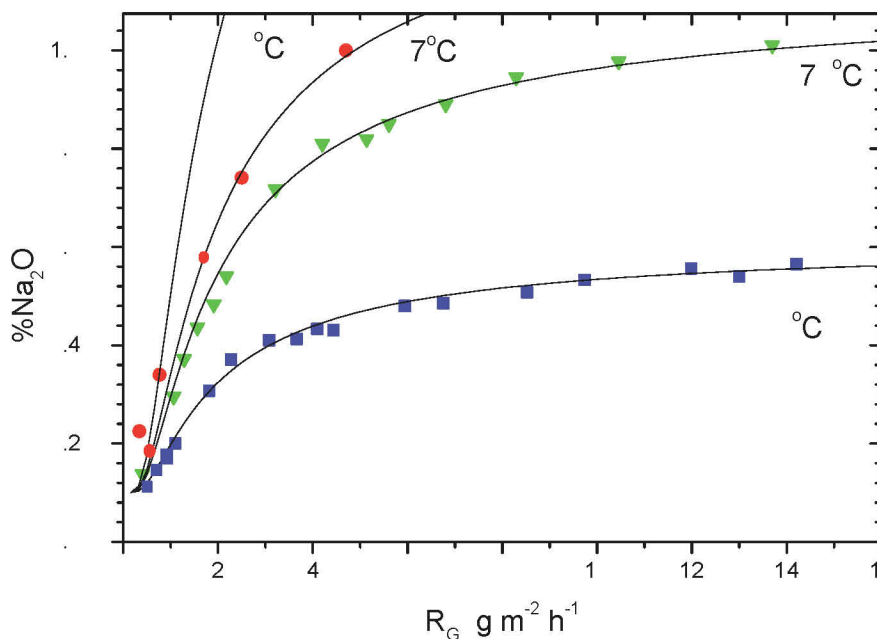


Figure 3. Experimental data (points) for soda incorporation into growing hydrate over a wide range of growth conditions and the best fit generated using Equation 5 (lines). The values of the parameters are listed in Table II. Soda is expressed in the conventional manner of percentage Na_2O in Al_2O_3 .

Equation 5 fits the data in Figure 3 very well. The parameters obtained from the best fit are shown in Table II. Two things are evident from Figure 3; (i) that sodium incorporation is a strong function of temperature for any given growth rate, and (ii) that sodium incorporation is a strong function of growth rate. The latter should be no surprise, as Sang [2] showed this with the use of supersaturation squared as the main factor in soda incorporation, and other authors have found similar supersaturation dependencies. The present work was purposely conducted over a large range of growth rates and temperatures in order to be able to distinguish each effect, but it can be seen from Figure 3 that in the region of most interest in alumina refining (that is, less than about $2 \text{ g m}^{-2} \text{ h}^{-1}$ growth rate and $70 \text{ }^\circ\text{C}$ to $60 \text{ }^\circ\text{C}$ temperature) it would be easy to overlook any temperature

dependence if that data were obtained in isolation, given the commonly experienced variability in determining $\% \text{Na}_2\text{O}$.

Table II. Values for parameters in Equation 5 after fitting to the data in Figure 3.

Parameter	Fitted value
k_{eq}	2.39×10^{-14}
E_{eq}	59 kJ mol^{-1}
K_{ads}	2.9×10^{-11}
E_{ads}	69.2 kJ mol^{-1}
R_c	$1.132 \text{ g m}^{-2} \text{ h}^{-1}$

Effect of Caustic Concentration

The effects of caustic concentration on soda incorporation were briefly studied by repeating a limited number of experiments at 70 °C using caustic concentrations of 150 and 250 g L⁻¹ Na₂CO₃. At low growth rates (up to 2 g m⁻² h⁻¹) there was no discernible effect of caustic concentration on soda incorporation as a function of growth rate. At higher growth rates in C 150 liquor, there were possible indications of decreased soda incorporation. In general though, it appears that there is little effect of caustic concentration on soda incorporation under the conditions encountered in alumina refineries.

Interpretation of the Fitted Parameters

Equation 5 is semi-empirical and the parameters in Table II should not be interpreted as fundamental properties, but they ought to at least correlate with recognizable crystal growth and surface chemistry phenomena if the equation is in fact a reasonable representation of the mechanism.

The first two parameters relating to the near-equilibrium case of very low growth rates are unlikely to have much meaning as the data has little dynamic range and the two effects cannot be separated. But the values are reasonable in terms of chemical kinetic processes. The value for E_{ads} in the “dynamic” part of the equation is again reasonable for chemical kinetics and is very similar to what would be expected of gibbsite crystal growth. This is in agreement that the soda incorporation mechanism, at a chemical level, is more than likely an inherent part of gibbsite growth.

The most interesting fitted parameter is the “critical growth rate” value, R_c , of 1.132 g m⁻² h⁻¹. This is easily converted into a linear growth rate of 0.47 μm h⁻¹. Lee’s data [15, 16] suggest that there is a significant dominance of the birth and spread mechanism at a calculated growth rate above approximately 0.45 μm h⁻¹. Although the change in mechanism is diffuse and difficult to establish with any certainty, it appears significant enough to hypothesize that whereas regular spiral growth will trap little sodium, birth and spread growth will trap a significant quantity of sodium by virtue of the higher proportion of defects produced.

Effect of Organics on Soda Incorporation

The effects of organics on soda uptake are well documented through the literature [5, 11-13, 20, 21]. If the hypothesis put forward in the present study is valid, it should be able to explain the effects of organics. To this end, several experiments were conducted in the presence of 100 ppm of sodium D,L tartrate. Tartrate, particularly the D,L form, is well known to poison gibbsite growth and increase soda uptake [21]. A level well below that known to completely poison growth was chosen. Figure 3 shows the result for growth at 70 °C, in C 200 liquor.

Tartrate clearly increases soda uptake to much higher levels at lower growth rates, but seems to leave the high-rate plateau the same. The effect is to steepen the curve, indicating that only the R_c variable is affected (decreased). The function describing the effect of organic poisons on R_c has not been fully explored, but it is expected that certain organics have the ability to increase the defect density generated for a given growth rate. It is important to

note that the defect density cannot exceed some upper limit, otherwise gibbsite is no longer formed. In experiments designed to increase the defect density by rapid precipitation at low temperatures, or at higher temperatures with increased supersaturation levels, phases other than gibbsite were precipitated.

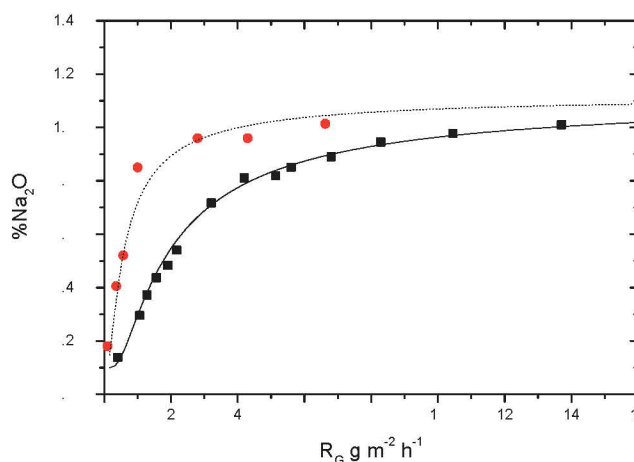


Figure 4. Soda incorporation as a function of growth rate at 70°C for pure synthetic liquor (■) and for identical liquor containing 100 ppm sodium D,L tartrate (●).

Observation of hydrate surfaces in the absence or presence of organics such as sodium tartrate show that at similar growth rates, hydrate grown in the presence of the organic has a much rougher appearance, indicating that birth and spread growth is more dominant. Figure 5 shows typical “poisoned” growth. This is not surprising; such organics are thought to retard hydrate growth through poisoning of the spiral steps. This leaves only birth and spread, which generates a greater proportion of sodium-trapping defects, as the main growth mechanism.

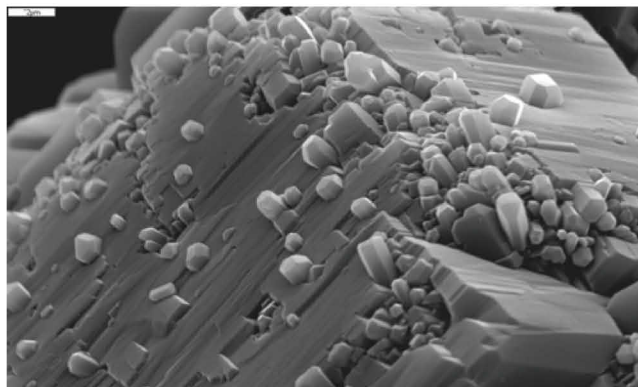


Figure 5. Hydrate (gibbsite) grown in the presence of 100 ppm sodium tartrate for 6 hours. Whereas hydrate grown in the absence of tartrate shows a smooth surface with step-like spreading growth, this sample shows multiple surface nucleation and rough non-epitaxial growth indicative of birth and spread as the dominant mechanism. The scale bar (top left) is 2 μm long.

Conclusions

It is hypothesized that soda incorporation involves trapping of sodium ions at defect sites, which are generated chiefly by the birth and spread mechanism. Certain classes of organic compounds increase sodium incorporation by altering the growth mechanism so that birth and spread is favored, probably by poisoning the more orderly spiral growth mechanism. Treatments of impurity trapping in the literature provide a basis for mathematical representation of the mechanism and a semi-empirical model was generated. The model's parameters are in general agreement with crystal growth phenomena.

Acknowledgements

The authors acknowledge the financial support of Alcoa World Alumina, Alcan, Pechiney, Queensland Alumina, BHP Billiton/Worsley Alumina and the AJ Parker Cooperative Research Centre. Much of this work was conducted as part of the Australian Minerals Industry Research Association (AMIRA) P625 project "Incorporation of Impurities during Gibbsite Precipitation". Thanks also to Prof. Gordon Parkinson for many useful discussions, Melissa Loan and Michael Zieba who contributed to the experimental program, and to Felicia Lee for allowing the reproduction of AFM images.

References

1. K. Wefers, "Zur Frage des Alkaligehaltes in Technischem Aluminiumhydroxid", *Z. Erzbergbau. Metall.*, 18 (1965), 459-463.
2. J.V. Sang, "Factors Affecting Residual Na₂O in Precipitation Products", *Light Metals*, 1988, 147-156.
3. N.I. Eremin, M.I. Cherepanova, N.S. Shmorgunencko and M.A. Maksakova, "The Nature of the Inclusion of Alkali Impurity in the Structure of Aluminium Hydroxide", *Soviet Non-Ferrous Metals Research*, 8 (1980), 132-135.
4. N.I. Eremin, M.I. Cherepanova and M.A. Maksakova, "Statistical Investigations into the Nature of the Inclusion of Alkali in the Structure of Aluminium Hydroxide Particles", *Soviet Non-Ferrous Metals Research*, 8 (1980), 263-266.
5. S.C. Grocott and S.P. Rosenberg, "Soda in Alumina. Possible Mechanisms for Soda Incorporation", *Proceedings of the International Alumina Quality Workshop (Gladstone, QLD)*, 1988, 271-287.
6. A.R. Gerson, "The Role of Fuzzy Interfaces in the Nucleation, Growth and Agglomeration of Aluminum Hydroxide in Concentrated Caustic Solutions", *Progress in Crystal Growth and Characterization of Materials*, 43 (2001), 187-220.
7. T. Radnai, P.M. May, G.T. Hefter and P. Sipos, "Structure of Aqueous Sodium Aluminate Solutions: a Solution X-Ray Diffraction Study", *Journal of Physical Chemistry A*, 102 (1998), 7841-7850.
8. P. Sipos, I. Bodi, P.M. May and G.Hefter, "Formation of NaOH⁰(aq) and Na[Al(OH)₄]⁰(aq) Ion Pairs in Concentrated Alkaline Aluminate Solutions", *Progress in Coordination and Organometallic Chemistry*, 1997, 303-308.
9. P. Sipos, S.G. Capewell, P.M. May, G. Hefter, G. Laurency, F. Lukacs, and R. Roulet, "Spectroscopic Studies of the Chemical Speciation in Concentrated Alkaline Aluminate Solutions", *Journal of the Chemical Society-Dalton Transactions*, 18 (1998), 3007-3012.
10. H.R. Watling, S.D. Fleming, W. van Bronswijk and A.L. Rohl, "Ionic Structure in Caustic Aluminate Solutions and the Precipitation of Gibbsite", *J. Am. Chem. Soc Dalton Trans.*, 18 (1998), 3911-3917.
11. P. Clerin and B. Cristol, "Contribution of Liquor Composition on Bound Soda", *Light Metals*, 1998, 141-146.
12. L. Armstrong, "Bound Soda Incorporation During Hydrate Precipitation", *Proceedings of the 3rd International Alumina Quality Workshop (Hunter Valley, NSW)*, 1993, 282-292.
13. L. Armstrong, J. Hunter, K. McCormick and H. Warren, "Bound Soda Incorporation During Hydrate Precipitation - Effects of Caustic, Temperature and Organics", *Light Metals*, 1996, 37-40.
14. C.F. Vernon, M.J. Brown, D. Lau and M.P. Zieba, "Mechanistic Investigations of Gibbsite Growth", *Proceedings of the 6th International Alumina Quality Workshop (Brisbane, Australia)*, 2002, 33-39.
15. M. Lee, *The mechanism of Gibbsite Crystal Growth in Bayer Liquors*, (PhD thesis, Curtin University of Technology, Perth, Western Australia, 1998).
16. M. Lee and G.M. Parkinson, "Growth Rates of Gibbsite Single Crystals determined using *in situ* Optical Microscopy", *J. Crystal Growth*, 199 (1999), 270-274.
17. J.D. Gale, A.L. Rohl, V. Milman and M.C. Warren, "An ab initio study of the Structure and Properties of Aluminum Hydroxide: Gibbsite and Bayerite", *Journal of Physical Chemistry B* 105 (2001), 10236-10242 .
18. R.N. Hall, "Segregation of Impurities during the Growth of Germanium and Silicon Crystals", *J. Phys. Chem.*, 57 (1953), 836-839.
19. A. Tsuchiyama, M. Kitamura and I. Sunagawa, "Distribution of elements in growth of (Ba,Pb)(NO₃)₂ crystals from the aqueous solution", *J. Cryst. Growth*, 55 (1981), 510-516.
20. W. van Bronswijk, H.R. Watling and Z. Yu. "A Study of the Adsorption of Acyclic Polyols on Hydrated Alumina", *Colloids and Surfaces A.*, 157 (1999), 85-94.
21. H.R. Watling, P.G. Smith, J. Loh, P. Crew, and M. Shaw, "Comparative Effects of Model Organic Compounds on Gibbsite Crystallisation", *Proceedings of the 4th International Alumina Quality Workshop (Darwin, Australia)*, 1996, 553-555.